1 **Colloid-bound and dissolved phosphorus species in topsoil water extracts along a grassland**

2 **transect from Cambisol to Stagnosol**

3 Xiaoqian Jiang[1], Roland Bol[1], Barbara J. Cade-Menun[2*], Volker Nischwitz[3], Sabine Willbold[3], Sara L.

4 Bauke[4], Harry Vereecken[1], Wulf Amelung[1,4], Erwin Klumpp[1]

5 [1] Institute of Bio- and Geosciences, Agrosphere Institute (IBG-3), Forschungszentrum Jülich GmbH,

6 Jülich, Germany

7 [2] Swift Current Research and Development Centre, Agriculture and Agri-Food Canada, Box 1030, 1

8 Airport Rd. Swift Current, SK, S9H 3X2 Canada

9 [3] Central Institute for Engineering, Electronics and Analytics, Analytics (ZEA-3), Forschungszentrum

10 Jülich GmbH, Jülich, Germany

11 [4] Institute of Crop Science and Resource Conservation, Soil Science and Soil Ecology, Nussallee 13,

12 University of Bonn, 53115 Bonn, Germany

14 *Corresponding author

15 Barbara J. Cade-Menun, Email: Barbara.Cade-Menun@AGR.GC.CA

Abstract

Phosphorus (P) species in colloidal and "dissolved" soil fractions may have different distributions. To understand which P species are potentially involved, we obtained water extracts from the surface soils of a gradient from Cambisol, Stagnic Cambisol to Stagnosol from temperate grassland, Germany. These were filtered to < 450 nm, and divided into three procedurally-defined fractions: small-sized colloids (20-450 nm), nano-sized colloids (1-20 nm), and "dissolved P" (< 1 nm), using asymmetric flow field flow fractionation (AF4), as well as filtration for solution ^{31}P-NMR spectroscopy. The total P of soil water extracts increased in the order Cambisol< Stagnic Cambisol< Stagnosol due to increasing contributions from the dissolved P fraction. Associations of C-Fe/Al-PO$_4^{3-}$/pyrophosphate were absent in nano-sized (1-20 nm) colloids from the Cambisol but not in the Stagnosol. The ^{31}P-NMR results indicated that this was accompanied by elevated portions of organic P in the order Cambisol > Stagnic Cambisol > Stagnosol. Across all soil types, elevated proportions of inositol hexakisphosphate species (e.g. *myo*-, *scyllo*-, and D-*chiro*-IHP) were associated with soil mineral particles (i.e. bulk soil and small-sized soil colloids) whereas other orthophosphate monoesters and phosphonates were found in the 'dissolved' P fraction. We conclude that P species composition varies among colloidal and "dissolved" soil fractions after characterization using advanced techniques, i.e. AF4 and NMR. Furthermore, stagnic properties affect P speciation and availability by potentially releasing dissolved inorganic and ester-bound P forms as well as nano-sized organic matter-Fe/Al-P colloids.

Keywords: colloidal phosphorus; dissolved phosphorus; field flow fractionation; ^{31}P-NMR; grassland; Cambisol; Stagnosol.

Abbreviations: AEP, 2-Aminoethyl phosphonic acid; AF4, asymmetric flow field flow fractionation; Al, aluminum; Ca, calcium; DNA, deoxyribonucleic acid; EDTA, Ethylenediaminetetraacetic; Fe, iron; FFF, field flow fractionation; ICP-MS, inductively coupled plasma mass spectrometer; myo-IHP, myo-inositol hexakisphosphate; N, nitrogen; NMR, nuclear magnetic resonance; OC, organic carbon; OCD, organic carbon detector; OM, organic matter; PES, polyethersulfone; Pi, inorganic P species; Po,

44 organic P species; Si, silicon; UV, ultraviolet; WDCs, water dispersible colloids; WDFCs, water

45 dispersible fine colloids.

46

1. Introduction

Phosphorus (P) is an essential nutrient for plant growth and limits terrestrial ecosystem productivity in many arable and grassland soils (Vance et al., 2003). The availability and transport of P depend on the speciation and concentration of P in the soil solution, which contains both 'dissolved' and colloidal P forms (Shand et al., 2000; Hens and Merckx, 2002; Toor and Sims, 2015). Dissolved orthophosphate is generally the main P species in solution and can be directly taken up by plant roots (Condron et al., 2005; Pierzynski et al., 2005). However, colloidal P in the size range of 1-1000 nm (Sinaj et al., 1998) may also contribute significantly to total P content in the soil solution (Haygarth et al., 1997; Shand et al., 2000; Hens and Merckx, 2001). Recent studies found that fine colloids (< 450 nm fraction) in soil water extracts consisted of nano-sized (< 20 nm) and small-sized (20 < d < 450 nm) particles with different organic matter and elemental composition (Henderson et al., 2012; Jiang et al., 2015a). Very fine nano-sized P colloids, around 5 nm are even prone to plant uptake (Carpita et al., 1979). In addition, the presence of fine colloids alters the free ionic P content in the soil solution through sorption processes (Montalvo et al. 2015). After diffusion-limited uptake depletes the free ionic P in the soil solution, these fine colloids disperse in the diffusion layer and therewith re-supply free ionic P species for roots (Montalvo et al., 2015). Because water-dispersible colloids (WDCs) can be easily released from soil in contact with water (Jiang et al., 2012; Rieckh et al., 2015), they have also been suggested as model compounds for mobile soil colloids (de Jonge et al., 2004; Sequaris et al., 2013). However, little is known about the chemical composition of P species in different-sized WDCs.

Recent studies have started to characterize natural fine colloidal P in freshwater samples and soil water extracts using asymmetric flow field flow fractionation (AF4) coupled to various detectors (e.g. ultraviolet [UV] and inductively coupled plasma mass spectrometer [ICP-MS]) for improved size fractionation of colloids and online analysis of their elemental composition (Henderson et al., 2012; Regelink et al., 2013; Gottselig et al., 2014; Jiang et al., 2015a). These analyses are increasingly combined with solution ^{31}P-nuclear magnetic resonance (NMR) spectroscopy, which offers low detection limits and can quantify different inorganic and organic P compound groups (Cade-Menun, 2005; Cade-Menun and Liu, 2014) in isolated colloidal materials (e.g. Liu et al., 2014; Jiang et al., 2015a, b; Missong et al., 2016). However, we are not aware of studies that have applied these methods

75 systematically to WDCs obtained from different major reference soils. Here, we focus on the

76 comparison of Cambisols and Stagnosols. In contrast to Cambisols, Stagnosols are soils with perched

77 water forming redoximorphic features. Due to temporary water saturation and resulting oxygen

78 limitation, the reduction of iron (Fe ^{III}) is accompanied by the dissolution of its oxides and hydroxides

79 (Rennert et al. 2014), and the P associated with these Fe-minerals should correspondingly be

80 redistributed in soil solution.

81 The objective of this study was to elucidate how stagnant water conditions alter the potential release of

82 different P compounds in colloidal and 'dissolved' fractions of soil solution. For this purpose, water-

83 extractable P was obtained from a transect of Cambisols to Stagnosols in a German temperate

84 grassland, and characterized using both solution ^{31}P-NMR and AF4 coupled online with UV and

85 organic carbon detector (OCD) or ICP-MS analyses.

86

87 **2. Materials and methods**

88 **2.1 Site description**

89 The grassland test site in Rollesbroich is located in the northern part of the Eifel in North Rhine-

90 Westphalia, Germany (50 ° 62 ´N, 06 ° 30 ´E). The grassland vegetation is dominated by perennial

91 ryegrass (*Lolium perenne* L.) and smooth meadow grass (*Poa pratensis* L.). According to the soil map

92 of the geological service of North Rhine-Westphalia (Fig. 1), the dominant soil types on the test site

93 are Cambisols (extensive meadow with three to four cuts per year, no cattle grazing), Stagnic

94 Cambisols (cattle pasture but with less frequent grazing than the Stagnosols), and Stagnosols

95 [intensively used as pasture with frequent cattle grazing followed by harrowing with a tire-drag harrow

96 and application of organic manure (cattle slurry)]; classification according to IUSS Working Group

97 WRB (2015). The elevation along the transect generally decreases from south to north, with the

98 highest elevation of 512.9 m a.s.l. at plot 1 and the lowest point of 505.1 m a.s.l. at plot 3 (Fig. 1,

99 Table 1). The catchment mean annual precipitation was 103.3 cm for the period from 1981 to 2001,

100 and the highest runoff occurred during winter due to high precipitation and low evapotranspiration

101 rates, as well as overland flow due to saturation excess (Gebler et al., 2015). The topsoil samples (2-15

102 cm) of plot 1 (S1-1, S1-2, and S1-3, Cambisol), 2 (S2, Stagnic Cambisol), and 3 (S3-1, S3-2, and S3-3,

103 Stagnosol) were taken as a representative transect across the site in early March, 2015 (Fig. 1). It is

104 worth noting that Stagnic water conditions do not mean that the soils are under reduced conditions for

105 the whole year – only for some significant time of the year. We sampled a Stagnosol, but only the

106 topsoil (2-15 cm) which was not under perching water, i.e., it was aerobic at time of sampling. As such,

107 the Stagnols used for this study were oxic at various times each year, but also experienced periods of

108 reducing conditions that did not occur in the other samples along the transect. Surface turf (0-2 cm)

109 was removed as it contained predominantly grass roots and little mineral soil. Removal of this very

110 surface turf may also help minimizing effects from recent manure input on soil properties. Stones and

111 large pieces of plant material were removed by hand. All samples were sieved immediately to < 5 mm

112 and stored at 5 ℃.

113

114 **2.2 Water dispersible fine colloids (WDFCs) separations and AF4-UV-ICP-MS / AF4-UV-OCD**

115 **analyses**

116 The WDCs of Rollesbroich grassland soil samples with three field replicates in S1 and S3 were

117 fractionated using the soil particle-size fractionation method of Séquaris and Lewandowski (2003), but

118 with moist soils. In brief, moist soil samples (100 g of dry soil basis) were suspended in ultrapure

119 water (Mill-Q, pH: 5.5) in a soil: solution mass ratio of 1:2, and shaken for 6 h. Thereafter, 600 mL of

120 ultrapure water were added and mixed. The WDCs suspensions were collected using a pipette after a

121 12-h sedimentation period. These WDCs suspensions were subsequently centrifuged for 15 min at

122 10,000 $\times$ g and filtered through 0.45-μm membranes (cellulose mixing ester) to produce the

123 suspension containing WDFCs sized below 0.45 μm. It is worth noting that Mill-Q water was used

124 here to extract soil colloids instead of rain water or pore water, since total amounts of WDFCs will

125 likely be larger when using Mill-Q water, i.e., we consider these WDFCs as potentially water-

126 dispersible colloids. In addition, the use of Mill-Q water facilitates subsequent sample processing with

127 AF4 and NMR. It is inevitable that Mill-Q water would result in the release of P due to desorption and

128 dissolution of poorly crystalline authigenic mineral phases. Additionally,living cells within the soil

129 would also certainly undergo significant osmotic stress, likely resulting in osmotic rupture and

130 releasing organic and inorganic P found in intracellular components. It is also worth noting that the

131 experimental procedure with Mill-Q water under oxic conditions may have an impact on oxidation of

132 aqueous iron (Fe^{2+}) and colloidal ferrous particles. However, at time of sampling, the very surface

133 soils were not fully water saturated as allowed even for Stagnosols for time of the year. As such, the

134 analyzed species and size fractions are representative of differences in response to the extraction

135 procedure based on different soil redox conditions that reflect a kind of legacy of former redox cycle,

136 but at time of sampling and analyses the soils were aerobic.

137

138 An AF4 system (Postnova, Landsberg, Germany) with a 1 kDa polyethersulfone (PES) membrane and

139 500 μm spacer was used for size-fractionation of the soil sample WDFCs. It is a separation technique

140 that provides a continuous separation of colloids. The retention time of the colloids can be converted

141 to hydrodynamic diameters of the colloids using AF4 theory or calibration with suitable standards

142 (Dubascoux et al., 2010). The AF4 was coupled online to an ICP-MS system (Agilent 7500, Agilent

143 Technologies, Japan) for monitoring of the Fe, aluminum (Al), silicon (Si), and P contents of the size-

144 separated particles (Nischwitz and Goenaga-Infante, 2012) and to OCD and UV detectors for

145 measuring organic carbon (OC). These elements were analyzed as part of the main soil minerals (e.g.

146 clay minerals and Fe oxides) that can be associated with P (Jiang et al., 2015a). The OCD is a

147 promising technique for monitoring OC concentrations for liquid-flow based separation systems with

148 the advantages of high selectivity and low detection limits (Nischwitz et al., 2016). Briefly, the

149 operation principle is that the acidification of the sample flow removes inorganic C and subsequently

150 the OC is oxidized in a thin film reactor to carbon dioxide, which can be quantified by infrared

151 detection (Nischwitz et al., 2016). A 25 μM NaCl solution at pH 5.5, which provided good separation

152 conditions for the WDFCs, served as the carrier. The injected sample volume was 0.5 mL and the

153 focusing time was 15 min with 2.5 mL min^{-1} cross flow for the AF4-UV-OCD system while 2 mL

154 injected volume and 25 min focusing time were used for the AF4-ICP-MS system. Thereafter, the

155 cross flow was maintained at 2.5 mL min^{-1} for the first 8 min of elution time, then set to decrease

156 linearly to 0.1 mL min^{-1} within 30 min, and maintained for 60 min. It then declined within 2 min to 0

157 mL min^{-1}, and remained at this rate for 20 min to elute the residual particles. The detection limit of the

158 ICP-MS system was 0.1-1 μg L^{-1} for the elements analyzed in this study. The AF4 characteristics of

159 WDFCs did not change significantly in the 6 months period of the investigation.

160

2.3 Particle separations of WDFCs and solution ^{31}P-NMR spectroscopy

162 The soil samples were treated as described in section 2.2 to obtain the suspension containing WDFCs

163 < 450 nm. We pooled the WDFCs suspensions of the field replicates in order to receive sufficient

164 samples for solution ^{31}P-NMR. The first peak fraction after AF4 separation has a particle size smaller

165 than ~20 nm (approximately 300 kDa; Jiang et al., 2015a; Fig. 2). Therefore, the suspension

166 containing WDFCs < 450 nm of these three samples were separated into three size fractions: 300 kDa-

167 450 nm, 3-300 kDa, and < 3 kDa (nominally 1 nm; Erickson, 2009). The 300 kDa-450 nm particle

168 fractions were separated by passing ~600 mL of the WDFCs suspension through a 300 kDa filter

169 (Sartorius, Germany) by centrifugation. The 3-300 kDa particle fractions were subsequently isolated

170 by passing the < 300 kDa supernatant through a 3 kDa filter (Millipore Amicon Ultra) by

171 centrifugation. Finally, the final supernatant containing the < 3 kDa particles as well as the electrolyte

172 phase was frozen and subsequently lyophilized.

173 The bulk soil samples (1 g) and the three fractions of soil water extracts were respectively mixed with

174 10 mL of a solution containing 0.25 M NaOH and 0.05 M Na$_2$EDTA (ethylenediaminetetraacetate) for

175 4 h, as a variation of the method developed to extract P for ^{31}P-NMR (Cade-Menun and Preston, 1996;

176 Cade-Menun and Liu, 2014; Liu et al., 2014). Extracts were centrifuged at 10,000 × g for 30 min and

177 the supernatant was frozen and lyophilized. Each NaOH-Na$_2$EDTA-treated lyophilized extract, and the

178 < 3 kDa fraction without NaOH-Na$_2$EDTA treatment, were dissolved in 0.05 mL of deuterium oxide

179 (D$_2$O) and 0.45 mL of a solution containing 1.0 M NaOH and 0.1 M Na$_2$EDTA (Turner et al. 2007).

180 A 10 μL aliquot of NaOD was added to the < 3 kDa fraction without NaOH-Na$_2$EDTA treatment to

181 adjust the pH. The prepared samples were centrifuged at 13,200 × g for 20 min (Centrifuge 5415R,

182 Eppendorf).

183 Solution ^{31}P-NMR spectra were obtained using a Bruker Avance 600-MHz spectrometer equipped

184 with a prodigy-probe (a broadband CryoProbe which uses nitrogen [N]-cooled RF coils and

185 preamplifiers to deliver a sensitivity enhancement over room temperature probes of a factor of 2 to 3

186   for X-nuclei from ^{15}N to ^{31}P), operating at 242.95 MHz for ^{31}P. Extracts were measured with a D_2O-

187   field lock at room temperature. Chemical shifts were referenced to 85% orthophosphoric acid (0 ppm).

188   The NMR parameters generally used were: 32 K data points, 3.6 s repetition delay, 0.7 s acquisition

189   time, 30 ° pulse width and 10,000 scans. Compounds were identified by their chemical shifts after the

190   orthophosphate peak in each spectrum was standardized to 6.0 ppm during processing (Cade-Menun et

191   al., 2010; Young et al., 2013). Peak areas were calculated by integration on spectra processed with 7

192   and 2 Hz line-broadening, using NUTS software (2000 edition; Acorn NMR, Livermore, CA) and

193   manual calculation. Peaks were identified as reported earlier (Cade-Menun, 2015), and by spiking a

194   select sample with myo-inositol hexakisphosphate (myo-IHP; McDowell et al., 2007).

195

196   **2.4 Statistical Analyses**

197   Elemental concentrations in bulk soils, soil water extracts, and AF4 fractograms of soil colloidal

198   particles were tested for significant differences (set to $P < 0.05$) using Sigmaplot version 12.5. A t-test

199   was conducted to determine the significance of differences among soil sites, whereas one-way

200   Repeated Measurements (RM) ANOVAs with Fisher LSD were performed with Fisher LSD post-hoc

201   test to test for significant differences among soil fractions and AF4 fractograms for the Cambisol and

202   Stagnosol. Data were assessed with Shapiro-Wilks and Brown-Forsythe-tests to meet the criteria of

203   normal distribution and homogeneity of variances respectively; those which had unequal variance data

204   were $\log_{10}$ transformed before statistical analyses.

205

206   **3. Results and discussion**

207   **3.1 Colloid and colloidal P distribution in different size fractions based on AF4-fractograms**

208   The AF4-UV-OCD and AF4-ICP-MS results of the WDFCs showed different OC, Si, P, Fe, and Al

209   concentrations in different-sized colloid fractions as a function of elution time (Fig. 2). Before the first

210   peak, an initial small void peak occurred at 1 min (Fig. 2 D, E, F). Thereafter, three different colloid-

211   size fractions occurred individually as three peaks in the WDFCs of all samples (Fig. 2). The first peak

212   of the fractograms corresponded to a particle size below 20 nm according to the calibration result

213   using latex standards (Jiang et al., 2015a). The third peak, which was eluted without cross flow,

214   contained only small amounts of residual particles or particles possibly previously attached on the

215   membrane during focus time; it had similar OC and element distributions as the second peak in all

216   samples (Fig. 2). Therefore we considered these two fractions together as a whole. As such, the size

217   ranges from 20 to 450 nm from here onward are described as the "second size fraction".

218   For the first fraction representing nano-sized colloids of the three field sites, the OCD and UV signals

219   indicated increasing OC concentration in the order of S1 (Cambisol; Fig. 2A), S2 (Stagnic Cambisol;

220   Fig. 2B), and S3 (Stagnosol; Fig. 2C). Distinct peaks of Fe, Al, and P in the first size fraction (< 20 nm)

221   were only present in the Stagnosol (S3; Fig. 2F), suggesting that under stagnant water conditions,

222   Fe/Al may more readily be involved in nano-sized soil particles than under other soil conditions. In

223   contrast, negligible amount of P, Al, and Fe were detected in the first fraction of S1 and S2 (Fig. 2D

224   and E, Table S1). While it is sometimes difficult to determine whether this peak is real or just the

225   tailing of the void signal (Fig. 2D and E), solution ^{31}P-NMR results confirmed the presence of P in this

226   size fraction (see next section). The nano-sized colloids from the Cambisol contained OC and

227   negligible P, Fe, and Al; those from the Stagnosol contained significantly higher concentrations of OC,

228   P, Fe, and Al (Table S1). We therefore assumed that the nano-sized colloidal P forms in the Stagnosol

229   mainly consisted of OC-Fe(Al)-P associations. Nanoparticulate humic (organic matter)-Fe (Al) (ions

230   /(hydr)oxide)-phosphate associations have recently been identified both in water and soil samples

231   (Gerke, 2010; Regelink et al., 2013; Jiang et al., 2015a). Our results suggest that the formation of these

232   nano-sized specific P-associations is favoured by the stagnant water conditions with high OC and

233   water contents in Stagnosol but not in the other soil types along the grassland transect.

234   The second size fraction (Fig. 2A, B, C, i.e. the small-sized colloids) contained significantly more OC

235   than the smaller nano-sized colloids for all studied soils (Table S1). Notably, the OC contents of the

236   second fraction increased in the order Cambisol < Stagnic Cambisol < Stagnosol; the UV signal

237   therein supporting the results obtained with the OC detector. The larger-sized colloids were

238   significantly richer in Al, Fe, Si, and P than the smaller-sized ones (Table S1), though again with

239   differences among subsites: the Stagnic Cambisol showed the largest Fe, Al, and Si contents in the

240   second fraction, as if there were a gradual change from low WDFC release in the Cambisol to the

241   formation of larger WDFC in the Stagnic Cambisol and finally to the formation of smaller WDFC in

242   the Stagnosol. Though this trend warrants verification by more sites, it appeared at least as if the

243   increasing oxygen limitation from Cambisols via Stagnic Cambisols to Stagnosols promoted an

244   increasing formation of small C-rich P-containing nanoparticles with additional contributions from Fe-

245   and Al-containing mineral phases. Stagnosols like S3 are characterized by a dynamic reduction regime

246   with dissolution of reactive Fe oxides (Rennert et al. 2014), which led to a decrease in the content of

247   Fe oxides in the second colloidal fraction (Table S1). Correspondingly, the dissolution of Fe oxides in

248   the second fraction under stagnant water may also liberate OC from the organo-Fe mineral

249   associations, thus releasing some OC to the nano-sized first fraction (Jiang et al., 2015a). This could

250   be an additional reason for the higher concentration of OC in the first peak of S3 (Table S1), apart

251   from a generally slower degradation of organic matter under limited oxygen supply (Rennert et al.

252   2014). Hence, the AF4 results indicated that the composition and distribution of particulate P varied

253   among the different-sized colloidal particles, and that its properties were impacted by the soil type and

254   related properties. However, AF4-ICP-MS results do not provide information about the elemental

255   concentrations of the 'dissolved' P fraction of these grassland soils. We cannot rule out any effects

256   from sample storage or from the use of Mill-Q water, as discussed in the Methods section, However,

257   although all samples were treated the same way, differences among the samples were consistent with

258   soil characteristics at each site. This suggests that the influences of treatment and storage were

259   minimal, but further investigation is warranted in future studies.

260

261   **3.2 Soil total, colloidal and dissolved P contents based on fractionation by filtration**

262   Soil water extracts < 450 nm, < 300 kDa, and < 3 kDa were obtained by filtration to determine total

263   elemental contents by ICP-MS analysis. Data did not have to be pooled for these analyses; as such, we

264   could test statistical differences. We considered the soil water extract < 3 kDa in this paper to be the

265   'dissolved' fraction. Significant differences ($P < 0.05$) were ascertained for elevated concentrations of

266   TOC, total P, as well for lower concentrations of total Al and Fe in the Stagnosol relative to the

267   Cambisol (Table 1). Furthermore, the Stagnosol had significantly higher concentrations of Si and P in

268   the individual size fractions of soil water extracts (except marginally significantly higher P in < 3 kDa,

269   $p = 0.06$), as well as higher Fe and Al concentrations in < 300 kDa and < 3kDa fractions than the

corresponding fractions of the Cambisol (Table 2). The Stagnic Cambisol generally resembled the Cambisol rather than the Stagnosol in bulk soil analysis, but this was not the case for the soil water extracts. This implied that the stagnic properties have a greater impact on the colloidal particles and "dissolved" fraction compared to bulk soil.

The oxygen limitation and reduction regime of the Stagnosol probably also favored the accumulation of OC and dissolution of Fe oxides both in bulk soil and colloids (Rennert et al. 2014). Dissolution of Fe oxides in turn results in a disaggregation of colloidal particles (Jiang et al., 2015a). As the released oxides are main carriers for P, these processes may explain why the distribution of colloidal and dissolved P also changed across the different grassland soils. As Table 2 shows, large proportions of P in the < 450 nm fraction of the Stagnosol were dissolved P (i.e. recovered here in the < 3 kDa fraction), whereas colloidal P dominated in the Cambisol and Stagnic Cambisol.

3.3 Inorganic and organic P species in the different-sized soil colloidal and the 'dissolved' fractions

Solution ^{31}P-NMR was used to elucidate the speciation of P in bulk soil and soil water extracts separated by ultrafiltration into the size fractions 300 kDa-450 nm, 3-300 kDa, and < 3 kDa for each of the three soils (Fig. 3 and S1, Table 3). The identified P included inorganic P forms (orthophosphate, pyrophosphate, and polyphosphate), and organic P in phosphonate, orthophosphate monoester and diester compound classes. Phosphonates included 2-aminoethyl phosphonic acid (AEP) and several unidentified peaks (Table S3). Orthophosphate monoesters included four stereoisomers of inositol hexakisphosphate (*myo-*, *scyllo-*, *neo-*, and D-*chiro*-IHP), diester degradation products (α-glycerophosphate, β-glycerophosphate and mononucleotides), choline phosphate, and unidentified peaks at 3.4, 4.2, 4.7, 5.0, 5.3, and 5.9 ppm. Orthophosphate diesters were divided into deoxyribonucleic acid (DNA) and two categories of unknown diesters (OthDi1 and OthDi2, respectively). Orthophosphate, pyrophosphate, orthophosphate monoesters, and diesters have also been detected in other studies of grassland, arable, and forest Cambisols and Stagnosols (e.g., Murphy et al., 2009; Turrion et al., 2010; Jarosch et al., 2015).

297   For the bulk soil samples and colloidal fractions of 300 kDa-450 nm of our soil samples,

298   orthophosphate and orthophosphate monoesters (mainly *myo*-IHP) were the main P compounds in all

299   samples (Fig. 3 and S1, Table 3 and S2). These main P compounds in these two soil fractions showed

300   similar trends among the soil samples: the proportions of organic P (e.g. orthophosphate monoesters

301   and diesters) decreased in the order of Cambisol > Stagnic Cambisol > Stagnosol (Table 3). The

302   similarity in this trend for the different organic P forms can likely be attributed to similarities in the

303   mineral components of bulk soil and colloidal fractions: i.e., similar element concentrations and thus

304   likely also similar clay mineralogy, Fe oxide signature and OC content of bulk soil and respective

305   colloid fraction according to the AF4-OCD and AF4-ICP-MS results (Fig. 2 and Table S1).

306   Orthophosphate, orthophosphate monoesters and diesters are predominantly stabilized by association

307   with these mineral components (Solomon and Lehmann, 2000; Turner et al., 2005; Jiang, et al, 2015a).

308   We assume that most of the relatively higher proportion of orthophosphate and lower percentage of

309   organic P in the Stagnosol may be attributed to the dissolution of Fe oxides, which likely released

310   organic P. Additionally, the higher concentrations of OC in both bulk soil (Table1) and large colloids

311   of the Stagnosol probably favored the formation of OC-Fe/Al-PO$_4^{3-}$ complexes (see above). However,

312   we cannot rule out the effects of differences in grazing and manure application on the P forms in these

313   soils. Cattle grazing and the application of cattle slurry would be expected to add P that is

314   predominantly orthophosphate, with lower concentrations of organic P forms including *myo*-IHP

315   (Cade-Menun 2011 and references therein). As such, this may have contributed to the increased

316   orthophosphate and decreased organic P we observed on these sites.

317   Our study is the first to distinguish the chemical P composition in colloidal fractions of 3-300 kDa and

318   300 kDa-450 nm. We found different P speciation and distribution between these two fractions. This is

319   probably related to differences in their element composition, which are dominated by OC-P/ OC-

320   Fe(Al)-P associations in the 3-300 kDa soil fraction and by clay-Fe oxides-OC-P associations in the

321   300 kDa-450 nm size fraction (Fig. 2). Intriguingly, we did not find any organic P but only inorganic P

322   in the 3-300 kDa of all three soils (orthophosphate in Cambisol and Stagnic Cambisol, orthophosphate

323   and pyrophosphate in the Stagnosol; Table 3). Furthermore, the Stagnosol nanoparticle fraction 3-300

324   kDa had a higher proportion of pyrophosphate than the 300 kDa-450 nm size fraction.

325 When comparing the solution ^{31}P-NMR results of the < 3 kDa soil fractions with and without NaOH-

326 Na$_2$EDTA treatments (Fig. 3 and Fig. S1), we observed that most of the phosphonates, orthophosphate

327 monoesters and diesters were lost after NaOH-Na$_2$EDTA treatment (Fig. 3 and Fig. S1). There were

328 two possible explanations: 1) 'dissolved' organic P in the NaOH-Na$_2$EDTA solution is sensitive and

329 easily hydrolyzed to orthophosphate (Cade-Menun and Liu, 2014); or 2) in absence of NaOH-

330 Na$_2$EDTA, most orthophosphate was removed by adsorption on sedimentary material in the re-

331 dissolved solution after centrifugation when preparing the samples for NMR analysis (Cade-Menun

332 and Liu, 2014), resulting in elevated portions of organic P in the NMR sample. The second possibility

333 may also explain the observation that there was no orthophosphate in the 'dissolved' fraction of the

334 Cambisol without NaOH-Na$_2$EDTA treatment (Fig. S1). Almost all the orthophosphate may have been

335 removed with the sedimentary phase due to the extremely low concentration of dissolved P in this soil.

336 Therefore, we will focus on the discussion of results obtained from the < 3 kDa soil fractions without

337 NaOH-Na$_2$EDTA treatment, as they provide better information on the origin of Po-species than the

338 other samples that received this treatment.

339 The composition of P species in the < 3 kDa soil fractions (i.e. "truly" dissolved P) differed among the

340 three soils (Table 3). The majority of observed P in the < 3 kDa soil fraction of the Cambisol was

341 organic P, comprised mainly of phosphonates and orthophosphate monoesters. The < 3 kDa soil

342 fraction of the Stagnic Cambisol contained various P species from all compound classes, including

343 orthophosphate, orthophosphate monoesters, orthophosphate diesters, pyrophosphate, polyphosphates,

344 and phosphonates. The < 3 kDa soil fraction of the Stagnosol contained similar P species as the

345 Stagnic Cambisol, with relatively higher proportions of orthophosphate monoesters and phosphonates,

346 but a lower proportion of orthophosphate diesters (Table 3). It is worth noting that there were more

347 species of phosphonates in the < 3 kDa fraction than other fractions of each soil (Fig. 3 and S1). The

348 larger signal at ~ 21-23.5 ppm was assigned to AEP (Doolette et al., 2009; Cade-Menun, 2015),

349 which occurred in both the soil particles and the < 3 kDa fraction. However, the small signals at ~ 36-

350 39 ppm and 45-46 ppm existed only in the < 3 kDa fraction of soil samples (Fig. 3 and S1). The

351 resonance at 36-39 ppm might be assigned to dimethyl methyl phosphonic acid, based on Cade-Menun

352   (2015). However, spiking experiments were not conducted to identify peaks in this region, so their

353   specific identity and origins remain unknown.

354   The solution ^{31}P-NMR results showed that P species composition in the two colloidal fractions and the

355   electrolyte phase differed among all three soil samples, with more phosphonates potentially existing in

356   the electrolyte phase. However, in the study of Missong et al. (2016), more phosphonates and

357   orthophosphate diesters were found in colloidal fractions rather than the electrolyte phase of two forest

358   Cambisols. Missong et al. (2016) used centrifugation while we used filtration to separate these particle

359   sizes and phases. Additionally, Missong et al. (2016) worked with forest soils while we worked with

360   grassland soils. McLaren et al. (2015) recently confirmed that the speciation of organic P is markedly

361   different between high (> 10 kDa) and low (< 10 kDa) molecular weight fractions of soil extracts. In

362   any case, both colloidal aggregation and changes in soil order paralleled P forms. However, also other

363   soil properties but former redox state (like pH), as well as variations in anthropogenic, site-adapted

364   management may be additional covariates affecting P colloids and composition.

365

366   **3.4 Distribution of orthophosphate monoesters and pyrophosphate**

367   With variations in overall P species composition, the proportions of certain species of orthophosphate

368   monoesters were also distributed differently among the investigated fractions of the three soils. For

369   example, the proportion of various IHP stereoisomers (i.e. *myo*-, *scyllo*-, D-*chiro*-IHP) decreased with

370   decreasing colloid size (Table S2). This suggests that the majority of IHP was associated with soil

371   mineral particles but did not exist in the dissolved form in our soil samples. The *myo*-IHP stereoisomer

372   is the principal input of inositol phosphate to soil in the form of plant material (Turner et al. 2002) and

373   the other stereoisomers may come from plants or may be synthesized by soil organisms (Caldwell and

374   Black, 1958; Giles et al., 2015). Inositol phosphate is stabilized mainly through strong adsorption on

375   the surface of amorphous metal oxides and clay minerals (Celi and Barberis, 2007). Shang et al. (1992)

376   found *myo*-IHP sorbed onto Al and Fe oxides to a greater extent than glucose 6-phosphate. Several

377   orthophosphate monoesters such as unknown peaks at 3.4, 4.7 and 5.9 ppm were only detected in the

378   electrolyte phase of soil samples (Table S2). The differences in orthophosphate monoester species

379   distribution between soil particles and the electrolyte phase show that soil minerals such as clay

minerals and Fe (Al) oxides are only associated with certain species of orthophosphate monoesters such as IHP, while other species of orthophosphate monoesters exist only in the electrolyte phase. Further research is warranted to fully understand the factors controlling Po in these different size fractions.

It is worth noting that although the proportion of pyrophosphate in bulk soil was very low, there was more pyrophosphate in the colloidal and electrolyte phases of the Stagnic Cambisol and the Stagnosol than in the Cambisol, and mostly in the electrolyte and nano-sized colloidal fraction (Table 3). Our former study (Jiang et al., 2015b) indicated that Fe/Al oxides were not the main bonding site for pyrophosphate adsorption in different-sized fractions of an arable soil. Considering that a high proportion of pyrophosphate (38.5%) existed in the 3-300 kDa fraction of the Stagnosol, which contained P mainly in OC-Fe(Al) $^{2/3+}$-P associations (see above), it seems reasonable to assume that pyrophosphate existed as a colloidal OC-Fe(Al)$^{2/3+}$-pyrophosphate complex. In this regard, the accumulation of pyrophosphate may have been favored by the larger OC contents in this soil (Fig. 2 C).

This study shows for the first time that P species composition varies among the electrolyte phase and colloids of different size, with the specific distribution being related to the stagnic water regime of the soil. It could potentially promote P availability by a mechanism that results in a loss of colloids, thus providing less surface area for the immediate bonding of inorganic P to minerals, while at the same time potentially releasing organic P from mineral bonding so that it is more prone to decomposition. Relating the static differences in P species composition among the different soils and fractions to true dynamics of P transformations, e.g., by performing controlled mesocosm experiments, now warrants further attention.

Appendix A. Supplementary data

The elemental concentrations in AF4 fractograms, phosphorus spectra and species determined by solution ^{31}P-NMR as well as solution ^{31}P-NMR chemical shifts of the P compounds were shown in supporting information.

Acknowledgments

X. Jiang thanks the China Scholarship Council (CSC) for financial support and acknowledges C. Walraf and H. Philipp for technical assistance. The authors gratefully acknowledge the support by TERENO (Terrestrial Environmental Observatories) funded by the Helmholtz Association of German Research Centers.

References

Cade-Menun, B.J., 2005. Characterizing phosphorus in environmental and agricultural samples by ^{31}P nuclear magnetic resonance spectroscopy. Talanta, 66, 359-371.

Cade-Menun, B.J. 2011. Characterizing phosphorus in animal waste with solution 31P NMR spectroscopy. pp. 275-299. In: Z. He, ed. Environmental Chemistry of Animal Manure. Nova Science Publishers, Inc. New York.

Cade-Menun B.J., 2015. Improved peak identification in ^{31}P-NMR spectra of environmental samples with a standardized method and peak library. Geoderma, 257-258, 102-114.

Cade-Menun, B.J., Carter, M.R., James, D.C., Liu, C.W., 2010. Phosphorus forms and chemistry in the soil profile under long-term conservation tillage: A phosphorus-31 nuclear magnetic resonance study. Journal of Environmental Quality, 39 (5), 1647-1656.

Cade-Menun, B.J., Liu, C.W., 2014. Solution ^{31}P-NMR spectroscopy of soils from 2005-2013, A review of sample preparation and experimental parameters. Soil Science Soceity of America Journal, 78, 19-37.

Cade-Menun, B.J., Preston, C.M., 1996. A comparison of soil extraction procedures for ^{31}P NMR spectroscopy. Soil Science, 161, 770-785.

Caldwell, A.G., Black, C.A., 1958. Inositol hexaphosphate. II. Synthesis by soil microorganisms. Soil Science Society of America Proceedings, 22, 293-296.

Carpita, N., Sabularse, D., Montezinos, D Delmer, D., 1979. Determination of the pore size of cell walls of living plant cells. Science, 205 (4411), 1144-1147.

Celi, L. Barberis, E., 2007. Abiotic reactions of inositol phosphatesin soil, in: Inositol Phosphates, Linking Agriculture and the Environment, edited by: Turner, B.L., Richardson, A.E., Mullaney, E.J., CAB International, Wallingford, UK, 207–220, 2007.

Condron, L.M., Turner B.L., and Cade-Menun B.J., 2005. Chemistry and dynamics of soil organic phosphorus. p. 87–121. *In* J.T. Sims, Sharpley A.N. (eds.) Phosphorus: Agriculture and the Environment. ASA, CSA, SSSA. Madison, WI.

de Jonge, L.W., Moldrup, P., Rubæk, G.H., Schelde, K., Djurhuus, J., 2004. Particle leaching and particle-facilitated transport of phosphorus at field scale. Vadose Zone Journal, 3 (2), 462-470.

Doolette, A.L., Smernik, R.J., and Dougherty, W.J., 2009. Spiking improved solution phosphorus-31 nuclear magnetic resonance identification of soil phosphorus compounds. Soil Science Soceity of America Journal, 73 (3), 919-927.

Dubascoux, S., Le Hecho, I., Hassellöv, M., v.d. Kammer, F., Gautier, M.P. and Lespes, G., 2010. Field-flow fractionation and inductively coupled plasma mass spectrometer coupling: history, development and applications. Journal of Analytical Atomic Spectrometry, 25(5), 613-623.

Erickson, H. P., 2009. Size and shape of protein molecules at the nanometer level determined by sedimentation, gel filtration, and electron microscopy. Biological Procedures Online, 11, 32–5.

449 Gebler, S., Hendricks Franssen H.J., Puetz T., Post H., Schmidt M., and Vereecken H., 2015. Actual
450   evapotranspiration and precipitation measured by lysimeters: a comparison with eddy covariance
451   and tipping bucket. Hydrol. Earth System Science, 19, 2145-2161.

452 Gerke, J., 2010. Humic (organic matter)-Al(Fe)-phosphate complexes: an underestimated phosphate
453   form in soils and source of plant-available phosphate. Soil Science, 175 (9), 417-425.

454 Giles, C.D., Lee L.G., Cade-Menun B.J., Hill J.E., Isles P.D.F., Schroth A.W., and Druschel G.K.,
455   2015. Characterization of organic phosphorus form and bioavailability in lake sediments using
456   ^{31}P NMR and enzymatic hydrolysis. Journal of Environmental Quality, 44: 882-894.

457 Gottselig, N., Bol, R., Nischwitz, V., Vereecken, H., Amelung, W., and Klumpp, E., 2014.
458   Distribution of phosphorus-containing fine colloids and nanoparticles in stream water of a forest
459   catchment. Vadose Zone Journal, 13 (7), 1-11.

460 Haygarth, P.M., Warwick, M.S., and House, W.A., 1997. Size distribution of colloidal molybdate
461   reactive phosphorus in river waters and soil solution. Water Research, 31 (3), 439-448.

462 Henderson, R., Kabengi, N., Mantripragada, N., Cabrera, M., Hassan, S., and Thompson, A., 2012.
463   Anoxia-induced release of colloid- and nanoparticle-bound phosphorus in grassland soils.
464   Environmental Science Technology, 46 (21), 11727-11734.

465 Hens, M. and Merckx, R., 2001. Functional characterization of colloidal phosphorus species in the soil
466   solution of sandy soils. Environmental Science Technology, 35 (3), 493-500.

467 Hens, M. and Merckx, R., 2002. The role of colloidal particles in the speciation and analysis of
468   "dissolved" phosphorus. Water Research, 36 (6), 1483-1492.

469 IUSS Working Group WRB. 2015. World Reference Base for Soil Resources 2014, update 2015.
470   International soil classification system for naming soils.

471 Jarosch, K.A., Doolette, A.L., Smernik, R.J., Tamburini, F., Frossard, E., and Bünemann, E.K., 2015.
472   Characterisation of soil organic phosphorus in NaOH-EDTA extracts: A comparison of ^{31}P NMR
473   spectroscopy and enzyme addition assays. Soil Biology and Biochemistry, 91, 298-309.

474 Jiang, C., Séquaris, J.-M., Vereecken, H., and Klumpp, E., 2012. Effects of inorganic and organic
475   anions on the stability of illite and quartz soil colloids in Na-, Ca- and mixed Na–Ca systems.
476   Colloids and Surfaces A: Physicochemical and Engineering Aspects, 415 (0), 134-141.

477 Jiang, X., Bol, R., Nischwitz, V., Siebers, N., Willbold, S., Vereecken, H., Amelung, W., and Klumpp,
478   E., 2015a. Phosphorus containing water dispersible nanoparticles in arable soil. Journal of
479   Environmental Quality, 44 (6), 1772-1781.

480 Jiang, X., Bol, R., Willbold, S., Vereecken, H., and Klumpp, E., 2015b. Speciation and distribution of
481   P associated with Fe and Al oxides in aggregate-sized fraction of an arable soil. Biogeosciences,
482   12 (21), 6443-6452.

483 Liu, J., Yang, J., Liang, X., Zhao, Y., Cade-Menun, B.J., and Hu, Y., 2014. Molecular speciation of
484   phosphorus present in readily dispersible colloids from agricultural soils. Soil Science Society of
485   America Journal, 78 (1), 47-53.

486   McDowell, R.W., Cade-Menun, B., and Stewart, I., 2007. Organic P speciation and pedogenesis:

487   analysis by ^{31}P nuclear magnetic resonance spectroscopy. European Journal of Soil Science, 58,

488   1348-1357.

489   McLaren, T.I., Smernik, R.J., McLaughlin, M.J., McBeath, T.M., Kirby, J.K., Simpson, R.J., Guppy,

490   C.N., Doolette A.L., and Richardson, A.E., 2015. Complex forms of soil organic phosphorus – A

491   major component of soil phosphorus. Environmental Science Technology, 49, 13238-13245.

492   Missong, A., Bol, R., Willbold, S., Siemens, J., and Klumpp, E., 2016. Phosphorus forms in forest soil

493   colloids as revealed by liquid-state ^{31}P-NMR. Journal of Plant Nutrition and Soil Science, 179 (2),

494   159-167.

495   Montalvo, D., Degryse, F., and McLaughlin, M.J., 2015. Natural colloidal P and its contribution to

496   plant P uptake. Environmental Science Technology, 49 (6), 3427-3434.

497   Murphy, P.N.C., Bell, A., and Turner, B.L., 2009. Phosphorus speciation in temperate basaltic

498   grassland soils by solution ^{31}P NMR spectroscopy. European Journal of Soil Science, 60, 638-651.

499   Nischwitz, V., and Goenaga-Infante, H., 2012. Improved sample preparation and quality control for

500   the characterisation of titanium dioxide nanoparticles in sunscreens using flow field flow

501   fractionation on-line with inductively coupled plasma mass spectrometry. Journal of Analytical

502   Atomic Spectrometry, 27 (7), 1084-1092.

503   Nischwitz, V., Gottselig, N., Missong, A., Meyn, T., and Klumpp, E. 2016 Field flow fractionation

504   online with ICP-MS as novel approach for the quantification of fine particulate carbon in stream

505   water samples and soil extracts. Journal of Analytical Atomic Spectrometry, 31, 1858-1868.

506   Pierzynski, G.M., McDowell, R.W., and Sims, J.T., 2005. Chemistry, cycling and potential movement

507   of inorganic phosphorus in soils. p. 53–86. *In* J.T. Sims, and A.N. Sharpley (eds.) Phosphorus:

508   agriculture and the environment. ASA, CSA, SSSA. Madison, WI.

509   Regelink, I.C., Koopmans, G.F., van der Salm, C., Weng, L., and van Riemsdijk, W.H., 2013.

510   Characterization of colloidal phosphorus species in drainage waters from a clay soil using

511   asymmetric flow field-flow fractionation. Journal of Environmental Quality, 42 (2), 464-473.

512   Rennert, T., Händel, M., Höschen, C., Lugmeier, J., Steffens, M., and Totsche, K.U., 2014. A

513   NanoSIMS study on the distribution of soil organic matter, iron and manganese in a nodule from

514   a Stagnosol. European Journal of Soil Science, 65 (5), 684-692.

515   Rieckh, H., Gerke, H.H., Glæsner, N., Kjaergaard, C., 2015. Tracer, dissolved organic carbon, and

516   colloid leaching from erosion-affected arable hillslope soils. Vadose Zone Journal, 14, 1539-1663.

517   Sequaris, J.M., Klumpp, E., and Vereecken, H., 2013. Colloidal properties and potential release of

518   water -dispersible colloids in an agricultural soil depth profile. Geoderma, 193-194, 94-101.

519   Séquaris, J.M., and Lewandowski, H., 2003. Physicochemical characterization of potential colloids

520   from agricultural topsoils. Colloids and Surfaces A: Physicochemical and Engineering Aspects,

521   217 (1-3), 93-99.

522 Shand, C.A., Smith, S., Edwards, A.C., and Fraser, A.R., 2000. Distribution of phosphorus in
523   particulate, colloidal and molecular-sized fractions of soil solution. Water Research, 34 (4), 1278-
524   1284.

525 Shang, C., Stewart, J.W.B., and Huang, P.M., 1992. pH effect on kinetics of adsorption of organic and
526   inorganic phosphates by short-range ordered aluminum and iron precipitates. Geoderma, 53 (1),
527   1-14.

528 Sinaj, S., Machler, F., Frossard, E., Faisse, C., Oberson, A., and Morel, C., 1998. Interference of
529   colloidal particles in the determination of orthophosphate concentrations in soil water extracts.
530   Communications in Soil Science and Plant Analysis, 29 (9-10), 1091-1105.

531 Solomon, D. and Lehmann, J., 2000. Loss of phosphorus from soil in semi-arid northern Tanzania as a
532   result of cropping: evidence from sequential extraction and ^{31}P-NMR spectroscopy. European
533   Journal of Soil Science, 51, 699-708.

534 Toor, G.S., and Sims, J.T., 2015. Managing phosphorus leaching in mid-Atlantic soils: importance
535 of legacy sources. Vadose Zone Journal, 14 (12), 1-12.

536 Turner, B. L., Cade-Menun, B. J., Condron, L. M., and Newman, S., 2005. Extraction of soil organic
537   phosphorus. Talanta, 66, 294-306.

538 Turner, B., Condron, L., Richardson, S., Peltzer, D., and Allison, V., 2007. Soil organic phosphorus
539   transformations during pedogenesis. Ecosystems, 10 (7), 1166-1181.

540 Turner, B.L., Papházy, M.J., Haygarth, P.M., and McKelvie, I.D., 2002. Inositol phosphates in the
541   environment. Philosophical Transactions of the Royal Society B Biological Sciences, 357 (1420),
542   449-469.

543 Turrion, M.B., Lafuente, F., Aroca, M.J., López, O., Mulas, R., and Ruipérez, C., 2010.
544   Characterization of soil phosphorus in a fire-affected forest Cambisol by chemical extractions and
545   ^{31}P-NMR spectroscopy analysis. Science of the Total Environment, 408 (16), 3342-3348.

546 Vance, C.P., Uhde-Stone, C., and Allan, D.L., 2003. Phosphorus acquisition and use: critical
547   adaptations by plants for securing a nonrenewable resource. New Phytologist, 157 (3), 423-447.

548 Young, E.O., Ross, D.S., Cade-Menun, B.J., Liu, C.W., 2013. Phosphorus speciation in riparian soils:
549   A phosphorus-31 nuclear magnetic resonance spectroscopy and enzyme hydrolysis study. Soil
550   Science Society of America Journal, 77 (5), 1636-1647.

551 Table 1 General soil characteristics and concentrations (g kg^{-1} soil) of total organic carbon (TOC), total Fe, Al, P, and Si in bulk S1 (Cambisol), S2 (Stagnic
552 Cambisol), and S3 (Stagnosol). The lowercase letters indicate significant differences among soil sites (significant difference of soil site 1 and 3 was tested by t-
553 test, $p < 0.05$).

Soil	pH[IV]	Water content (%)	Elevation (m a.s.l.)	TOC (g kg^{-1})	Fe*(g kg^{-1})	Al (g kg^{-1})	P (g kg^{-1})	Si (g kg^{-1})
S1[I]	4.90±0.12a	46.5±2.9	512.9	35.6±2.3a*	23.0±1.1a*	52.6±2.9a	1.2±0.1a	320±7.6
S2[II]	4.90	45.3	507.5	35.8	24.0±0.4	54.0±2.0	1.3±0.1	320±7.0
S3[III]	5.36±0.20b	59.0±7.6	505.1	71.1±15.1b*	12.8±0.4b*	38.7±1.1b	1.8±0.4b	312±12.1

554 [I] The mean of sample S1-1, S1-2, and S1-3 ±standard deviation.
555 [II] The mean of three replicate sample S2 ±standard deviation.
556 [III] The mean of sample S3-1, S3-2, and S3-3 ±standard deviation.
557 [IV] The mass ratio of soil : water = 1:2.5.
558 * Data were log transformed before t-test analyses because of unequal variances.

Table 2 Concentrations (mg kg^{-1} soil) of P, Al, Fe, and Si in soil water extracts < 450 nm, < 300 kDa, and < 3 kDa, respectively. Different lowercase and uppercase indicate significant differences among soil sites and soil fractions, respectively (significant difference of soil sites 1 and 3 was tested by t-test, One Way RM ANOVA for soil fractions with Fisher LSD post-hoc test, P <0.05).

Soil	DOC (g kg^{-1})	P (mg kg^{-1})			Al (mg kg^{-1})			Fe (mg kg^{-1})			Si (mg kg^{-1})		
	< 450 nm	<450nm	<300kDa	<3kDa	<450nm	<300kDa	<3kDa	<450nm	<300kDa	<3kDa	<450nm	<300kDa	<3kDa
S1[I]	0.18	0.3±0.1a*	0.2±0.2a*	0.1±0.1	2.0±0.4A°	0.6±0.0$^{\alpha}$aB°	0.6±0.0$^{\alpha}$aB°	2.1±0.5A	0.2±0.0$^{\alpha}$aB	0.2±0.0$^{\alpha}$a*B	8.1±0.6aA	6.8±0.3aB	6.6±0.4aB
S2[II]	0.17	1.3±0.9	0.5±0.6	0.4±0.3	7.3±0.3	1.1±0.2	1.1±0.2	9.2±0.5	0.4±0.1	0.4±0.1	14.1±0.5	7.3±0.0$^{\alpha}$	7.8±0.8
S3[III]	0.23	4.4±2.0b*	3.3±2.7b*	4.1±2.6	4.1±3.1	0.7±0.1b	0.7±0.0b	4.6±3.3	0.4±0.1b	0.5±0.1b*	14.6±1.3b	10.6±2.1b	11.4±2.5b

[I] The mean of sample S1-1, S1-2, and S1-3 (Cambisol) ± standard deviation.

[II] The mean of three replicate extracts of sample S2 (Stagnic Cambisol) ± standard deviation.

[III] The mean of sample S3-1, S3-2, and S3-3 (Stagnosol) ± standard deviation.

$^{\alpha}$ Standard deviation of 0.0 means value <0.05.

*Data were log transformed before t-test analyses because of unequal variances.

°Data were log transformed before One Way RM ANOVA analyses because of unequal variances.

568 Table 3 the proportion (%) of phosphorus species[a] determined by solution ^{31}P-NMR for the different soil fractions of S1 (Cambisol), S2 (Stagnic Cambisol), and
569 S3 (Stagnosol).

Soil fractions	Pi	Po	Ortho-P	Pyro-P	poly	P-mono	P-mono*	P-diest	P-diest*	Phon-P
						---------%				
S1 bulk	43.4	56.6	41.2	1.5	0.7	52.9	44.5	2.2	10.6	1.5
S2 bulk	47.8	52.2	46.4	0.9	0.5	48.6	43.7	1.4	6.3	2.2
S3 bulk	63.7	36.3	63.0	0.2	0.5	31.2	27.0	1.5	5.7	3.6
S1 300 kDa-450 nm	22.8	77.2	22.8	-[ɣ]	-	56.7	49.5	11.1	18.3	9.4
S2 300 kDa-450 nm	56.8	43.2	53.1	1.0	2.7	29.9	26.9	5.2	8.2	8.1
S3 300 kDa-450 nm	70.2	29.8	59.7	9.2	1.3	24.2	19.9	2.8	7.1	2.8
S1 3-300 kDa	100	-	100	-	-	-	-	-	-	-
S2 3-300 kDa	100	-	100	-	-	-	-	-	-	-
S3 3-300 kDa	100	-	61.5	38.5	-	-	-	-	-	-
S1 < 3 kDa	13.5	86.5	-	-	13.5	26.9	26.9	1.9	1.9	57.7
S2 < 3 kDa	21.3	78.7	9.5	5.1	6.7	29.3	13.8	24.2	34.6	25.2
S3 < 3 kDa	22.2	77.8	8.8	6.0	7.4	29.4	27.4	8.2	10.2	40.2

570 [a] inorganic P (P$_i$), organic P (P$_o$), orthophosphate (Ortho-P), pyrophosphate (Pyro-P), polyphosphate (poly), orthophosphate monoesters (P-mono),
571 orthophosphate diesters (P-diest), phosphonates (Phon-P). * recalculation by including diester degradation products (α glycerophosphate, β glycerophosphate, and
572 mononucleotides) with P-diest rather than P-mono (Liu et al. 2014; Young et al. 2013). ᵞ below detection limit, i.e. <0.05%.

573
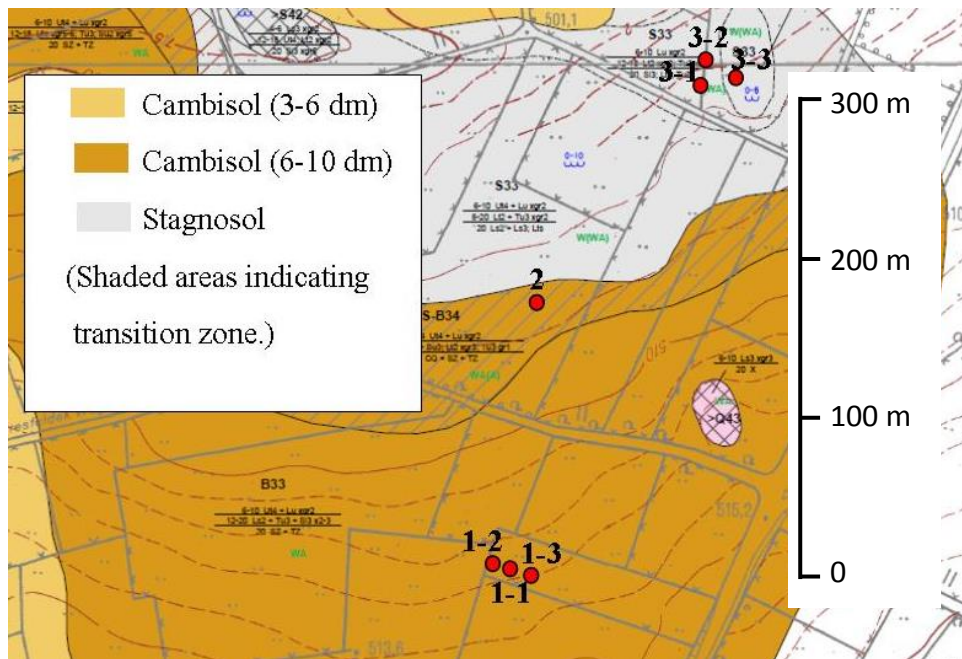
574

575   Fig. 1 Excerpt from the soil map of the test site at Rollesbroich (*modified from Geologischer Dienst*

576   *Nordrhein-Westfalen, 2008*). Numbered red dots indicate location of plots.

577

578

579
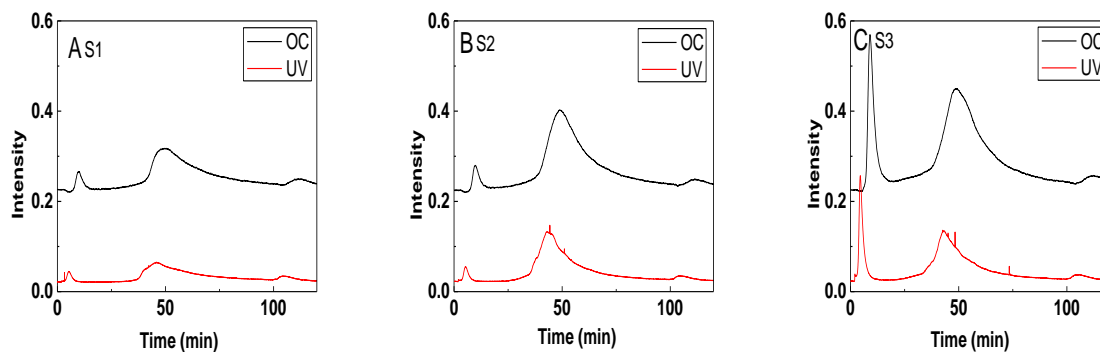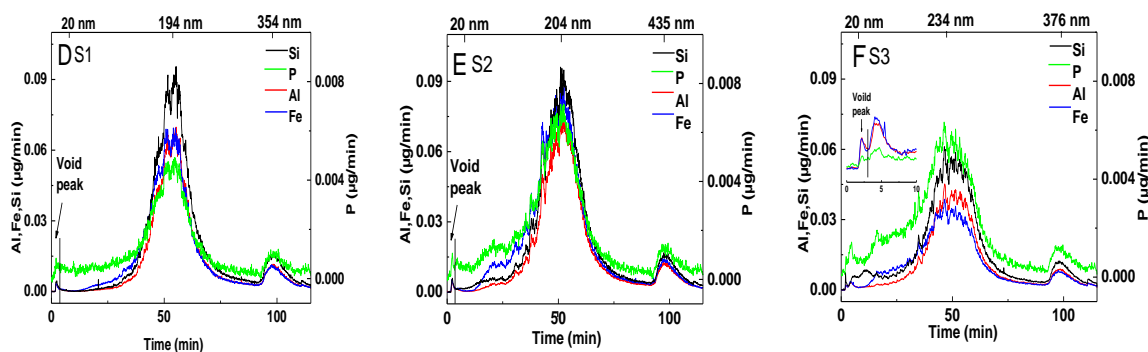
Fig. 2 Asymmetric flow field-flow fractionation (AF4) fractograms of water dispersible fine colloids (WDFCs) of S1, S2, and S3. The fractograms show the organic carbon (OC) and ultraviolet (UV) signal intensities (A, B, and C) and the Fe, Al, P, and Si mass flow (D, E, and F) monitored by inductively coupled plasma mass spectrometer (ICP-MS) of S1 (Cambisol), S2 (Stagnic Cambisol), and S3 (Stagnosol). The sizes of peaks were according to the AF4 result of sulfate latex standard particles and dynamic light scattering results. The OC and UV peaks occurred with elements (ICP-MS) peaks at the same time and the slight delay among these peaks is due to the different length of tubes to different detectors which cause slightly different internal volume and retention time.

588

589

590

591

592

593

594

595
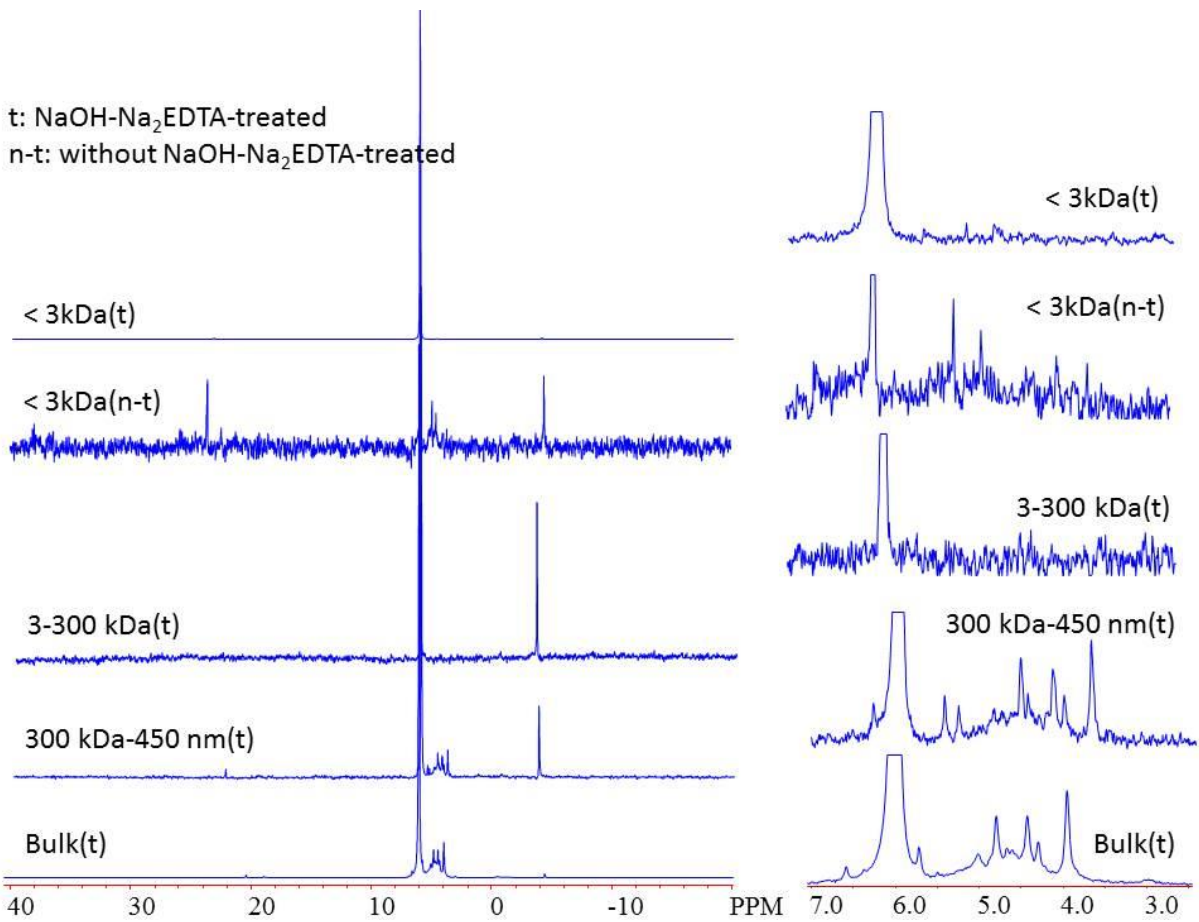
Fig. 3 Solution phosphorus-31 nuclear magnetic resonance spectra of NaOH–Na$_2$EDTA extracts of

bulk soil, 300 kDa-450 nm, 3-300 kDa and < 3 kDa fractions in soil water extracts < 450 nm of S3

(Stagnosol).

599

600